wjert, 2024, Vol. 10 Issue 4, 97-122. Original Article ISSN 2454-695X

World Journal of Engineering Research and Technology
WJERT
www.wjert.org

SJIF Impact Factor: 5.924

SPILLWAY SURFACE PROTECTION FROM CAVITATION DAMAGES

Novikova Inna* and Kupriyanov Vladimir

JSC "Institute Hydroproject", 2, Volokolamskoe shosse, Moscow, 125993, Russian Federation.

Article Received on 09/02/2024 **Article Revised on 29/02/2024** **Article Accepted on 19/03/2024**

***Corresponding Author**
Novikova Inna
JSC "Institute Hydroproject", 2, Volokolamskoe shosse, Moscow, 125993, Russian Federation.

ABSTRACT

The damage caused by cavitation is a significant issue for high-head spillways. Examples have been cited where the extent of damage was so substantial that further operation of the spillways without restoration became impossible. Existing methodologies for detecting cavitation risk in spillway structures rely on average water flow velocities, leading to inflated requirements for permissible velocities. This article presents the results of the authors' laboratory research on the conditions of appearance and progression cavitation behind offsets of varying heights. Cavitation index was calculated based on fixed pressures and velocities in the boundary layer at offset height. The theory of ideal liquid jets was applied to convert cavitation indices, recorded in limited-size cavitation chambers, into indices applicable to unbounded natural flow. Visual observations of cavitation cavity development with increasing velocities enabled the identification of the most hazardous cavitation phases. Recommendations are provided for safeguarding spillways against cavitation damage, taking into account the impact of hydrodynamic pressure, flow velocity in the boundary layer at offset height, material strength, flow surface aeration, and the duration of water flow.

KEYWORDS: Spillways, Cavitation, Damages, Velocity, Surface irregularities, Offset into flow.

1. INTRODUCTION

In hydraulic engineering structures, especially those with water velocities exceeding 25-30 m/s, the issue of ensuring cavitation safety in spillways becomes highly relevant. Similar to how sound and thermal "barriers" posed challenges for achieving high speeds in atmospheric travel, cavitation represents a "barrier" for attaining high water flow velocities in hydraulic structures.

Cavitation occurs in areas of reduced pressure, such as on gate elements, gate chambers, flow energy dissipators, deep spillway intakes, flow turning sections, on surface irregularities of the spillway, and others. For hydraulic structures, the danger lies not in cavitation itself but in the damage it can induce (Falvey, 1990). Initially, cavitation-induced damages are localized and do not affect the operation of the spillway. However, over time, they can escalate significantly, leading to operational difficulties and even the breach of the hydraulic structure's pressure front.

Figures 1-5 illustrate some examples of substantial cavitation-induced damages, wherein continued operation of spillways without restorative repairs becomes impossible (Borden *et al.*, 1971; Semenkov, 1979; Kenn & Garrod, 1981; Burgi *et al.*, 1984; Houston *et al.*; 1985; Falvey, 1990; Voynov *et al.*, 1998; Rajasekhar *et al*., 2014; Oroville Dam, 2018).

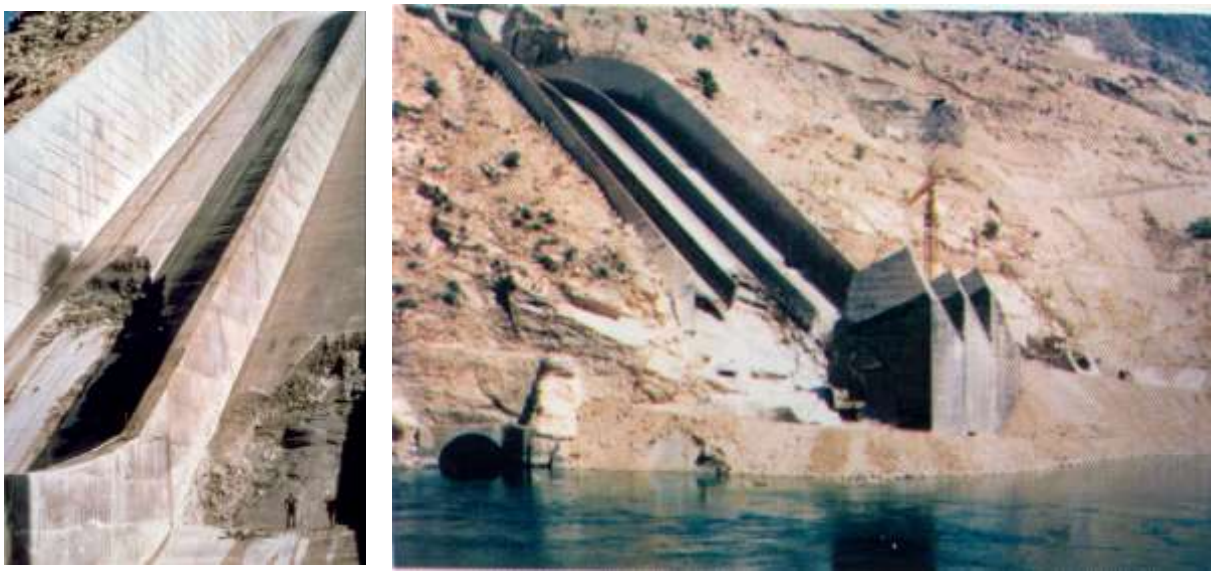

a) **b)**

Figure 1: Karun-1 (Shahid Abbaspour) Dam (Iran). Cavitation-induced damages to the operational spillway in 1993: a – initial stage of damage (Terrier, 2016); b - central and right spans destroyed, their foundation displaced, and damage to the toe blocks of the piers (Voynov et al., 1998).

a) **b)**

Figure 2: Oroville Dam (USA). Spillway chute damage (Oroville Dam, 2018): a - This initial erosion hole at the service spillway was examined by a climb team on the morning of February 8, 2017; b - Ultimate damage at the service spillway.

a) **b)**

Figure 3: Nagarjuna Sagar Dam (India): a - erosion of spillway during the floods of 2009; b - cavitation damage on dam (Rajasekhar et al., 2014).

Figure 4: Sayano-Shushenskaya HPP (Russia). Construction spillway of the second tier. Cavitation-induced damages to the floor and sidewalls behind the gate chamber (1980).

a) **b)**

Figure 5: Bureyskaya HPP (Russia). Construction deep spillway, bottom orifice No. 7 (2005): a - right edge (length of concrete damage approximately 12 m); b - left edge (length of concrete damage approximately 18 m).

Modeling studies and operational experience with spillway dams such as Grand Coulee (USA), Bratskya Hydroelectric Power Plant (Russia), Sup'ung (China), construction spillways of the Sayano-Shushenskaya Hydroelectric Power Plant (Russia), tunnel spillways

like Yellowtail, Boulder (USA), and others have demonstrated that increasing water flow velocities lead to a sharp increase in cavitation impact on the flow. The intensity of cavitation erosion is proportional to the velocity raised to the power of 5…7. This implies that with an increase in the spillway height, for example, from 50 to 100 m, the intensity of cavitation erosion increases by 6…11 times, and from 50 to 150 m, it increases by 16…45 times.

Factors determining the possibility of cavitation erosion on the surface of a spillway structure include the location and size of the source creating the zone of reduced pressure, water flow velocity, cavitation phases, air content in the water, duration of continuous water discharge, and the resistance of the lining material to cavitation impact.

The degree of cavitation development is determined by the cavitation index. The cavitation index σ characterizes the ratio of forces resisting the continuity rupture in the moving flow to the forces promoting such rupture. Forces resisting continuity rupture can be expressed as the excess of absolute pressure P_0 over vapor pressure P_v at some characteristic point. Forces promoting fluid rupture are characterized by the flow's kinematic state and can be expressed as the velocity head $\rho V_0^2/2$. Thus, the cavitation index σ can analytically be expressed as the ratio

$$\sigma = \frac{P_0 - P_v}{\frac{\rho V_0^2}{2}}, \qquad (1)$$

Where P_0 and V_0 are the pressure and velocity at a characteristic point, P_v is the vapor pressure, and ρ is the density of water.

Critical conditions for incipient of cavitation are characterized σ_i, where σ_i is inception cavitation index. The degree of cavitation development (its phase) is characterized by the relative cavitation index (σ/σ_i) and the relative length of the cavitation cavity (l/z).

The extent of damage of any surface, caused by cavitation is not constant with time. Observations have shown that several different rates actually occur. Each rate has been given a specific name. At first, a period begins, where loss of material does not occur. This period is known as the "incubation zone." In this zone, damage is insignificant and can be acceptable.

The purpose this investigation

- Systematize laboratory data on cavitation indexes for their application in natural flow condition;
- Identify the most damage cavitation phases;
- Develop a methodology for determining the permissible height of isolated irregularities on the spillway surface to prevent cavitation damage.

2. MATERIALS AND METHODS

Studied critical conditions for cavitation appearance on surface irregularities in hydrodynamic pipes (Colgate, 1972; Ball, 1975; Arndt *et al.*, 1979; Jin *et al.*, 1985). Determined critical indexes of incipient cavitation (σ_i) for the isolated irregularities of different forms. In various research laboratories, the working chambers of cavitation stands had their specific dimensions. Thus, in studies of Colgate (1972) the working section was 152 mm wide and 76 mm high, while in studies of Jin *et al.* (1985) the working section was 200×200 mm in size. Holl (Arnd *et al.*, 1979) determined the incipient cavitation indexes of isolated plane irregularities in the turbulent boundary layer on the plane plate located on the pipe axis. Performed his programmed work in two hydrodynamic pipes of University of Pennsylvania, 120 mm and 305 mm in diameter. The results of studies by some authors of the hydraulic conditions of the incipient cavitation occurrence on the surface roughness shown in Figure 6.

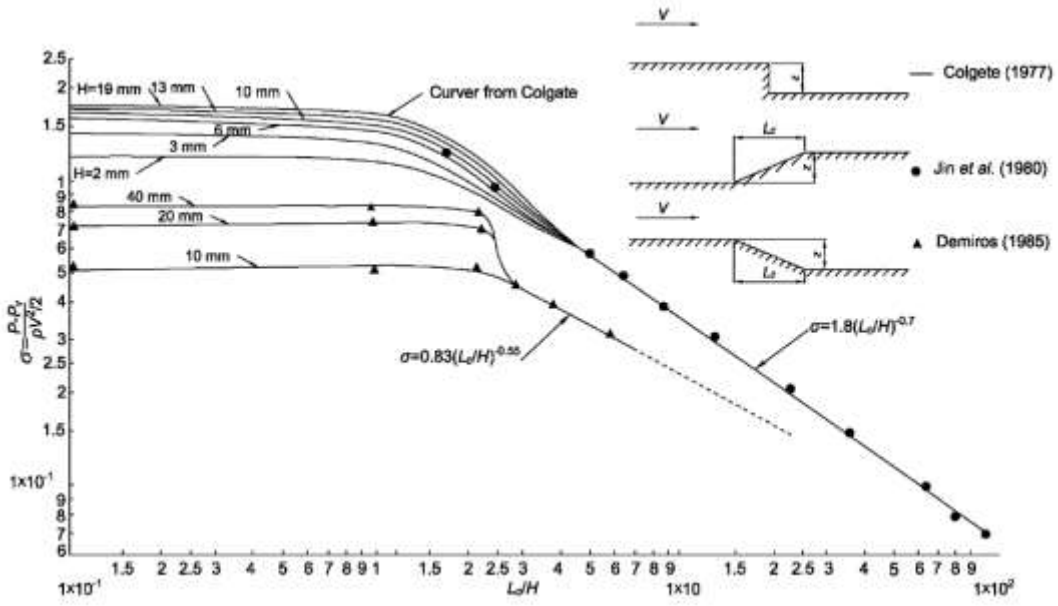

Figure 6: Cavitation characteristics of chamfers (Falvey, 1990).

The presented dependencies in Figure 6 are valid only for flows with a similar ratio between the height of a singular roughness element *z* and the thickness of the boundary layer δ, as well as the ratio between the boundary layer thickness and the flow depth. The question of generalizing these results for the analysis of cavitation situations in natural flows remained open. Results obtained in different laboratories lacked correlation, and the characteristic protrusion (Figure 6) in the height dependency exhibited different values of incipient cavitation index σ_i. The selection of a characteristic point for determining P_0 and V_0 is crucial, as the presence of a boundary layer and flow constriction caused by the roughness model in the cavitation chamber of the hydrodynamic tube influences the calculated cavitation index.

Relations presented in the Figures are true only for the flows with similar ratio between the single irregularity height *z* and boundary layer thickness δ and ratio between the boundary layer thickness and flow depth δ/B. Results obtained in different laboratories not correlated. The representative offset of different heights (Figure 6) had different means of incipient cavitation index σ_i. The question of the obtained results generalization for the analysis of the cavitation situation in the natural flow remained open. Selection of the characteristic point for determining P_0 and V_0 is fundamental, since the presence of a boundary layer and restriction of flow by the model irregularity in the working chamber of hydrodynamic pipe influenced the design value of the cavitation index.

Research the incipience cavitation and its development was conducted in the laboratory of Scientific and Research Centre of Hydroproject (Moscow, Russia) in two hydrodynamic pipes. The working chambers sections were 92 mm×35 mm and 250 mm×35 mm in size. The relative offset height z/B varied from 0.013 to 0.267.

The theory of ideal liquid jets was applied to convert cavitation indexes, recorded in limited-size cavitation chambers, into indexes applicable to unbounded natural flow (Berman, 1995).

Data on the incubation period for concrete of the deferent strength are obtained during the operation of spillway dams Krasnoyarsk and Bratsk of hydroelectric power stations.(Galperin *et al.*,1977).

The prevalent methodology currently utilized to assess cavitation risk on spillway surfaces considers solely the cavitation index, which is proposed to be calculated based on the average

velocity and pressure within the water flow. (Best Practices, 2019). It is assumed that significant damage will not occur if the cavitation index σ exceeds 0.5. Serious cavitation surface damage is deemed possible for cavitation indexes ranging from 0.5 to 0.2. This recommendation implies that cavitation damage may occur on spillway surfaces at water flow velocities between 23 m/s and 36 m/s.

For instance, Kermani *et al.* (2013, 2018) investigated the potential occurrence of cavitation damage on the spillway surface of the Korun-1 (Shahid Abbaspour Dam). They considered the average water flow velocity and cavitation index at various sections along the spillway length. A classification of the Level of Cavitation Damage was presented, establishing five danger levels corresponding to different flow velocities and cavitation indexes. Calculated cavitation index values were provided for the entire curved section of the Korun-1 spillway at various discharge rates. Downstream, these values σ decreased from 0.4 to 0.1. According to the adopted methodology, cavitation damage to the surface was anticipated along the entire length of the spillway. In reality, only the lower part of the spillway was damaged, as shown in Figure 1.

Wan *et al.* (2018) and Echávez (2021) assert that, when identifying cavitation-induced damage risk zones, it is crucial to examine flow characteristics near the conduit surface, where the phenomenon occurs, rather than averaging across conduit sections. Cavitation indices, calculated based on velocity and pressure near the surface, should be compared with initial indices of irregularities formed on the surface during construction works. Attention should be paid to compliance with the structure's profile, the presence of convex and concave surfaces, skewness, axis displacements, as well as the existence of protrusions and recesses. Echávez (2021) argues that the contingency in the Oroville Dam (USA) serves as an illustrative example highlighting the critical importance of the issue. The initial cause of the damage was a convexity in the profile, leading to a zone of negative pressure.

The presence of an advanced cavitation phase and a low cavitation index value is a necessary but insufficient condition for the occurrence of cavitation damage on the spillway surface. An additional condition involves the presence of a flow velocity capable of damaging the surface, considering the material strength of the facing, the degree of water flow aeration, and the duration of discharge flows. Only by considering these conditions can one reliably predict potential surface damage on the spillway.

3. RESULTS

3.1. Systematization of data by incipient cavitation indexes

In the analysis of results obtained in hydrodynamic tubes, the crucial factor is the selection of a characteristic section for calculating the index of cavitation inception, denoted as σ_i.

Figure 7 depicts the kinematic structure of the flow near a two-dimensional offset with a height of *z*, situated in the working chamber of a cavitation setup, with a limited chamber height *B*. In this scenario, cavitation occurs at the point of minimum pressure *M*, located within the detached vortex layer. The minimum pressure on the axis of the vortex layer is determined by the pressure in the compressed section of the chamber and the velocity at the outer boundary of the vortex layer V_j. Accordingly, in the systematization of laboratory research data on incipient cavitation indexes σ_i, the characteristic velocity V_0 should be considered as the velocity at the boundary of the vortex wake V_j, and the characteristic pressure P_0 should be regarded as the pressure in the compressed section downstream of the offset.

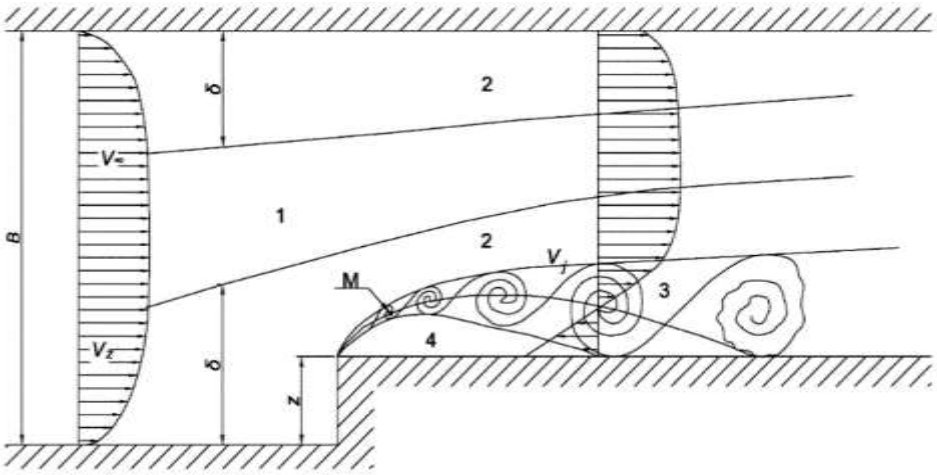

Figure 7: Flow pattern around a rectangular offset.

1 - potential core, 2 - boundary layer, 3 - turbulent vortex wake, 4 - recirculation zone.

The theory of an ideal liquid jet was employed to convert cavitation index values of individual irregularities in the laboratory to indices of the same irregularities in the boundary layer of a natural flow. Numerous theoretical works have focused on the influence of flow boundaries on supercavitating flows (Efros, 1946; Gilbarg & Rock, 1946; Birkhoff *et al.*, 1950). Birkhoff *et al.* (1950) demonstrated that when a flat plate is surrounded by a channel flow, the drag coefficient C_x can have nearly constant values if the characteristic velocity is

taken as the velocity at the boundary of the jet flow V_j around the plate, rather than the velocity in the approaching flow V_∞. According to this proposed method, V_j/V_∞ it is possible to determine the cavitation indexes of the jet flow of an ideal, weightless liquid

$$\frac{V_j}{V_\infty} = \sqrt{\sigma_j^\infty + 1}, \qquad (2)$$

Where V_j velocity at the boundary of the cavitation cavity; V_∞ velocity in the core of the approaching flow; σ_j^∞ cavitation index of the jet flow, where $V_0 = V_\infty$.

The problem of super cavitation (jet) flow around offset on the channel bottom in an ideal liquid was solved by Berman & Novikova (1995). In the considered scheme, the cavitation cavity forms above the upper boundary of the protrusion. The incoming flow at an infinitely remote point *A* has a velocity V_∞, parallel to the channel walls. For super cavitation flows, when the relative length of the cavity, $L/z \to \infty$ denoted as, a dependency $\sigma_j = f(B/z)$ was derived, as presented in Figure 8.

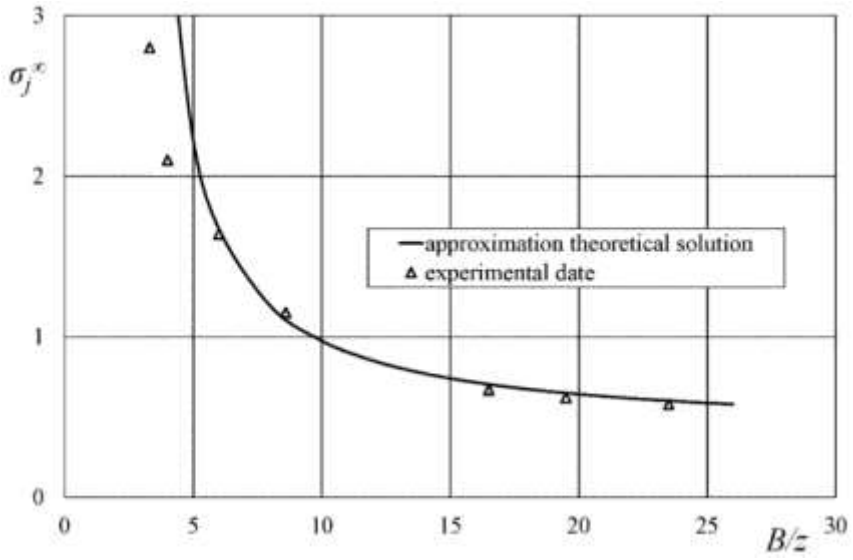

Figure 8: Comparison of analytical and experimental results for jet flow past a rectangular offset on the channel bottom (Berman & Novikova, 1995).

The obtained relationship is approximated by the formula

$$\sigma_j^\infty = 0.4 + \frac{4.2}{\left(\frac{B}{z} - 2.7\right)}, \qquad (3)$$

where σ_i^∞ cavitation index for jet flow; B height of the chamber; z height of the offset. When $B/z \to \infty$, $\sigma_j^\infty \to 0{,}4$ and according to (2) $V_j/V_\infty = \sqrt{1.4}$. For jet flows, the interface between the continuous liquid and the vapor and gas region is stable, with a constant velocity on it.

At the Hydropower Research Institute (Moscow, Russia), laboratory studies on the conditions of cavitation cavity inception and development were conducted. Figure 9 shows that in experiments, the cavitation onset index for a rectangular offset facing the flow σ_i^∞ varies from 0.4 to 2.6, if the characteristic velocity V_∞ and pressure P_∞ in the core of the incoming flow are considered in formula (1).

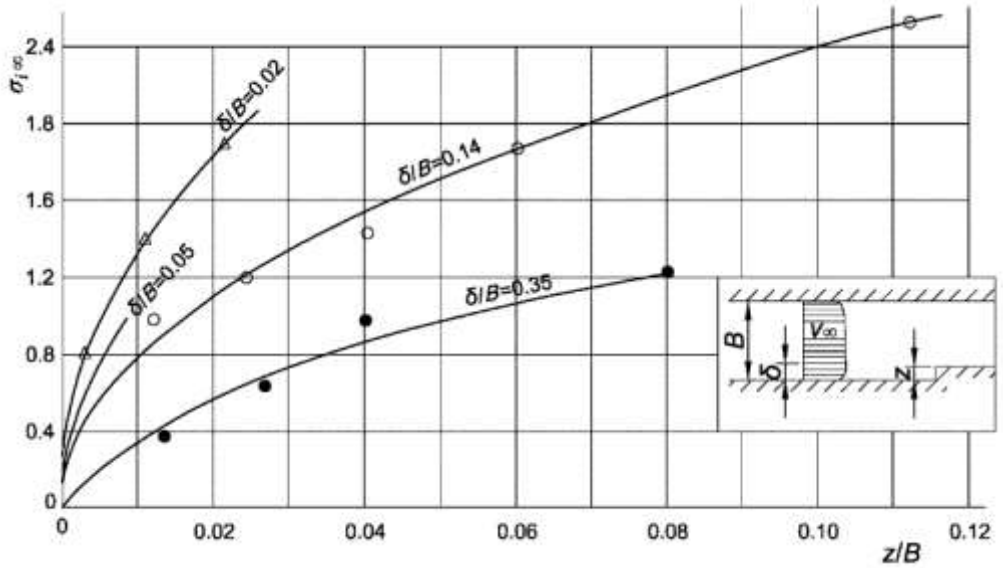

Figure 9: Dependency of the incipient cavitation index σ_i for a straight offset, calculated based on the velocity in the flow core, on the relative height of the offset z and the boundary layer thickness δ.

The value σ_i^∞ changes depending on the constriction of the working chamber by the protrusion and the ratio z/δ, where δ is the boundary layer thickness. The conducted research showed that the influence of the boundary layer on the cavitation index can be eliminated by taking the velocity in the boundary layer at the top of the offset V_∞^z as the characteristic velocity. However, the constriction of the working chamber by the offset continues to affect the magnitude $\sigma_i^{z\infty}$ (Figure 10).

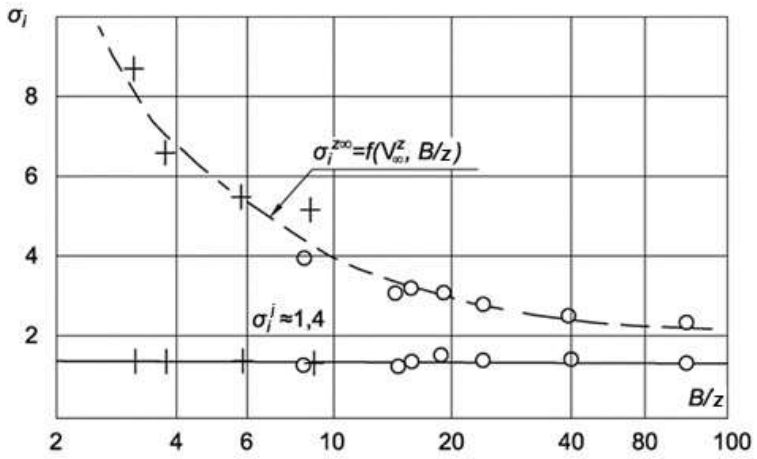

Figure 10: Dependence of the incipient cavitation index $\sigma_i^{z\infty}$, σ_i^j, upon the relative width B/z for a rectangular offset on the channel bottom (Berman & Novikova, 1995).

The incipient cavitation index will have a unique value for all B/z ratios only if the characteristic velocity V_j at the boundary of the vortex sheet behind the offset is considered. In the case of a rectangular protrusion facing the flow (Figure 10), incipient cavitation index will be equal to

$$\sigma_i^j = \frac{P_j - P_v}{\frac{\rho V_j^2}{2}} = 1.4. \qquad (4)$$

For a single irregularity on the surface of a natural watercourse, when $B/z \to \infty$ approaches infinity, the incipient cavitation index takes almost constant value if the characteristic stream is taken as the stream in the approaching flow before the offset, and the characteristic velocity as the velocity in the boundary layer at the top of the offset V_∞^z. Then, using relationships (2) and (4), we get

$$\sigma_i^{z\infty} = \sigma_i^j \left(\frac{V_j}{V_\infty^z}\right)^2 = 1.96. \qquad (5)$$

3.2. Advanced phases of cavitation and intensity of cavitation erosion

The degree of cavitation development (its phase) is characterized by the relative cavitation index σ/σ_i and the relative length of the cavitation cavity L/z. The experimental dependence $L/z = f(\sigma/\sigma_i)$ is shown in Figure 11. Here, σ is the cavitation index reflecting hydraulic conditions for the source of cavitation in the flow, σ_i is inception cavitation index for this

source, z is the characteristic linear size of the cavitation source, and L is the length of the cavitation cavity.

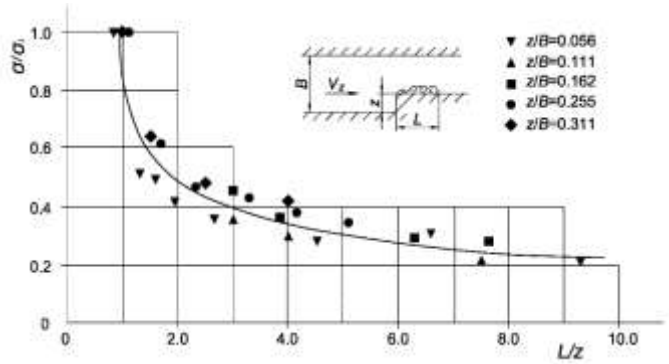

Figure 11: Dependency of the relative cavitation index on the length of the cavitation region for a rectangular offset.

Visual observations of the cavitation zone structure (Figure 12) have shown that when a offset is subjected to high-speed flow, various flow regimes can occur depending on the relative cavitation index σ/σ_i, where is the index of an arbitrary cavitation phases σ, and is the cavitation inception index σ_i. Cavitation behind the rectangular offset occurs on the axis of the vortex formed near the sharp edge at a distance $L/z \approx 0.75$, where z is the height of the offset.

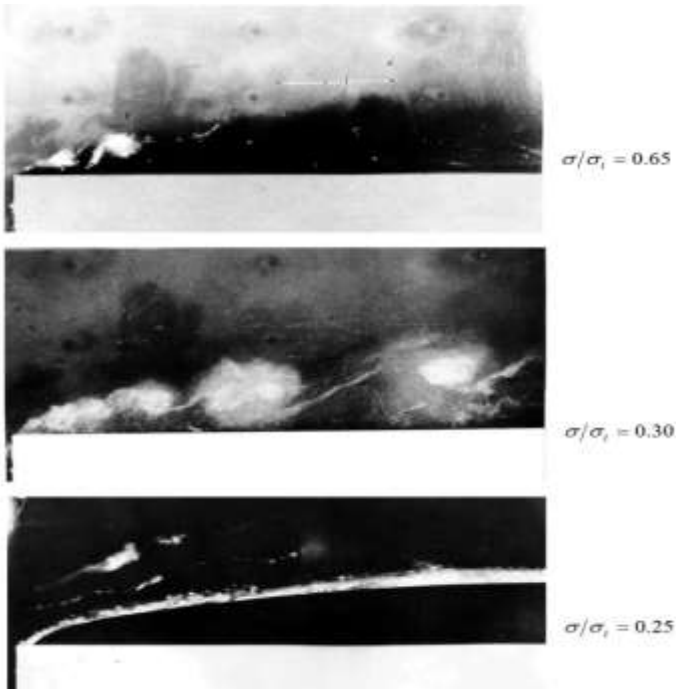

Figure 12: Development of the cavitation zone behind a rectangular offset into flow.

In the initial phase of cavitation with $\sigma/\sigma_i > 0.51$ ($\sigma > 1.0$), cavitation bubbles are located only in the zone of the mixing vortex layer, which does not come into contact with the surface of the upper edge of the offset. During these stages, cavitation cannot cause surface damage. When $0.45 \le \sigma/\sigma_i \le 0.51$, the cavitation vortex trail closes on the surface at a distance L/z = 1.4-2.5, and the area and intensity of surface damage are insignificant. In subsequent stages of cavitation, when $\sigma/\sigma_i < 0.45$ ($\sigma < 0.88$), a non-stationary cavity forms that closes on the edge of the protrusion, and its length increases as the cavitation indices decrease. When $\sigma/\sigma_i < 0.12$ ($\sigma < 0.23$), there is a jet (super-cavitational) flow, during which the flow completely detaches from the surface being covered, and no damage occurs.

The maximum intensity of cavitation erosion behind the rectangular offset is observed at $\sigma/\sigma_i = 0.25 \div 0.35$ ($\sigma = 0.5 \div 0.7$) (Figure 13).

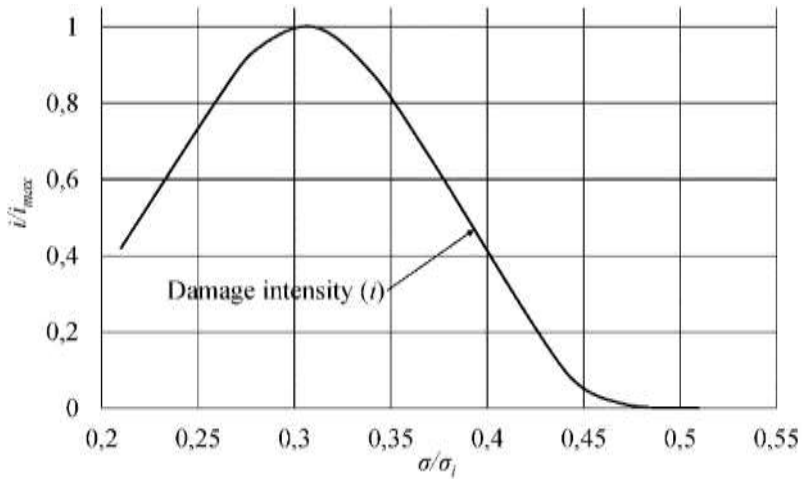

Figure 13: Relation between i/i_{max} ***and*** σ/σ_i

The dependence of cavitation danger level on the cavitation index for a rectangular offset facing the flow (formwork offset, welded seam, etc.) is presented in Table 1.

Where σ –is the calculated cavitation index in the real flow for height z of the allowable offset. The cavity does not reach the surface and can.t damage it, when $\sigma > \sigma_{cr} = 1.0$. σ_{cr} =1.0 – cavitation index for the incipient of damage.

For cavitation indexes, the characteristic velocity is not the average flow velocity, but the local velocity at the height offset *z*. In most cases, $V_z < \overline{V}$, so using average velocities in calculations leads to a significant exaggeration of cavitation danger.

To find the velocity V_z, it is necessary to first determine the type of flow on the considered section. Conditionally, in each spillway hydraulic structure, three characteristic sections can be distinguished (Figure 14).

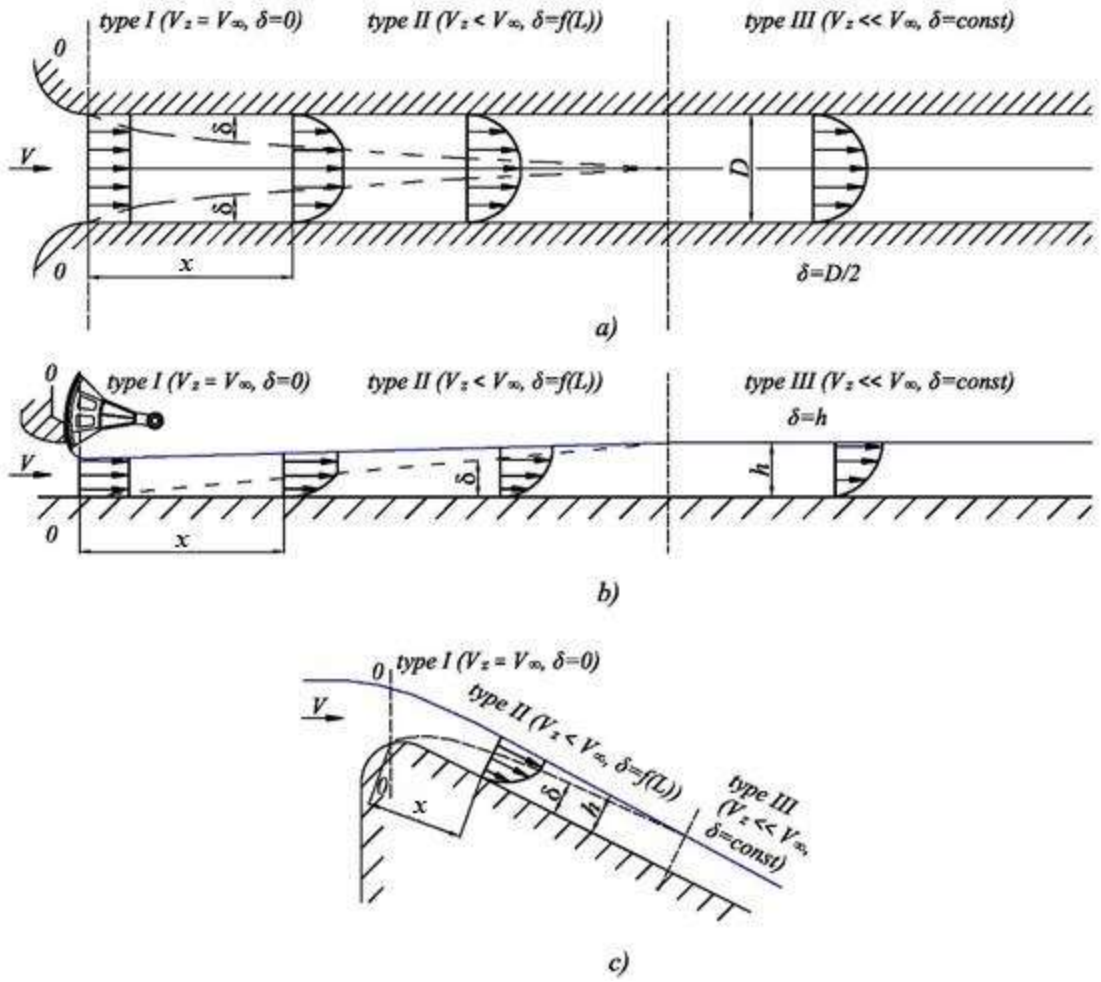

Figure 14: Typical flow regions in hydraulic engineering structures: a – tunnel; b – chute; c – spillway dam.

- Sections of sharp flow deformation according to the structure (inlets, turns, flow compression behind the gate, flow around separate piers, etc.) (Type I);
- Initial sections of smoothly changing flow with a growing boundary layer δ (pressure and free-flow tunnels, spillway surfaces of dams, fast flows) (Type II);
- Sections of smoothly changing flow with an established velocity distribution across the flow section (final sections of long pressure and free-flow conduits) (Type III).

On sections of the first type, the boundary layer is practically absent, so it can be conditionally assumed that for these sections $V_z = \overline{V}$, where $\overline{V}$ is the average velocity in the section.

On sections of the second type, the boundary layer grows, and the velocity near the wall decreases. In this case, many authors (Chanson, 1994; Chow, 2009) suggest using a power-law for determining the velocity at the height of the roughness

$$\frac{V}{V_{\max}} = \left(\frac{z}{\delta}\right)^{\frac{1}{N}}, \qquad 0 < z/\delta < 1.0 \qquad (6)$$

Several formulas exist for determining the boundary layer thickness depending on the length of the initial section x

$$\frac{\delta}{x} = 0.024\left(\frac{x}{k_S}\right)^{-0.13}, \qquad \text{(Bauer, 1954)} \qquad (7)$$

here, k_s represents the equivalent uniform sand grain absolute roughness.

$$\frac{\delta}{x} = 0.0212(\sin\theta)^{0.11}\left(\frac{x}{k_S}\right)^{-0.10}, \qquad \text{(Wood, 1983)} \qquad (8)$$

here, θ denotes the angle of inclination of the spillway surface to the horizontal.

$$\frac{\delta}{x} = 0.08\left(\frac{x}{k_S}\right)^{-0.233} \qquad \text{(Khatsuria, 2005)} \qquad (9)$$

Using the power-law to determine V_z leads to significant errors as there is no exact formula for δ and the exponent N = 4-10 in formula (6) changes depending on surface roughness and Reynolds number.

It is proposed to use the logarithmic law of velocity distribution by Karman-Prandtl (Schlichting & Gersten, 2017) for constructing the velocity diagram in the design section and determining the velocity magnitude at height z

$$V_z = u_*\left(8.5 + 5.75\lg\frac{z}{k_S}\right) \qquad (10)$$

For initial sections with growing boundary layers, the dynamic velocity u_* is determined by formula (Schlichting & Gersten, 2017)

$$\frac{u_*}{V_\infty} = \frac{1}{2}\sqrt{\left(2.87+1.58\lg\frac{x}{k_S}\right)^{-2.5}} \qquad (11)$$

On sections of the third type, where the movement is uniform, and the boundary layer thickness is constant, the velocity V_z is also determined by the logarithmic formula (10). The dynamic velocity for uniform flow in the spillway can be determined by the formula

$$\frac{u_*}{V} = \sqrt{\frac{\lambda}{8}}, \qquad (12)$$

where λ Darcy's coefficient.

3.3. Incubation period and critical velocity

The presence of a developed cavitation phase behind a single roughness on the surface is not a sufficient condition for the appearance of cavitation erosion on the surface. Another necessary condition is $V_z > V_{cr}$, where V_{cr} is the critical velocity at which initial surface damage may occur on a specific material after the incubation period T_{inc}. Observations have shown that several different rates of erosion occur. At first, a period begins where loss of material does not occur. It is known as the incubation period. Laboratory data on critical velocity for concretes of various strengths and different air content in the wall layer with an incubation period of T_{inc} = 48 hours are shown in Figure 15.

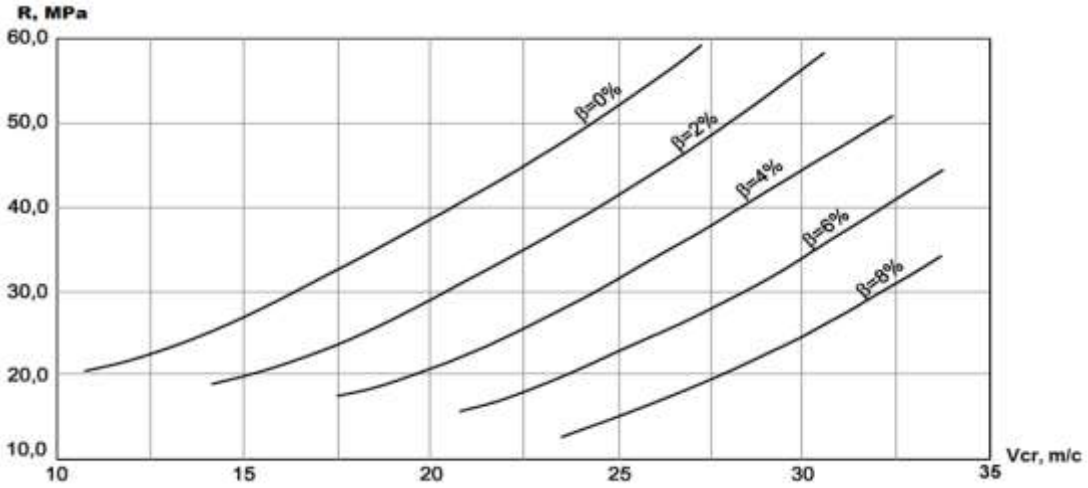

Figure 15: Dependence of critical water flow velocity on compressive strength and aeration of the wall layer for an incubation period of 48 hours. (Novikova et al, 1976, 1995).

These data allow determining the required strength of concrete based on the actual flow velocity at the height of the roughness and the air content in the wall area. . Correspondingly, for an incubation period different from 48 hours (Figure 16), the critical velocity is determined by the formula:

$$V_{cr} = V_{cr}^{*}\left(\frac{T_{inc}^{*}}{T_{inc}}\right)^{0.1}, \qquad (13)$$

is V_{cr}^{*} the critical velocity at the normalized incubation period T_{inc}^{*} = =48 hours, and T_{inc} is the calculated incubation period for the considered object. It is recommended to take it equal to the duration of a flood with 50% assurance.

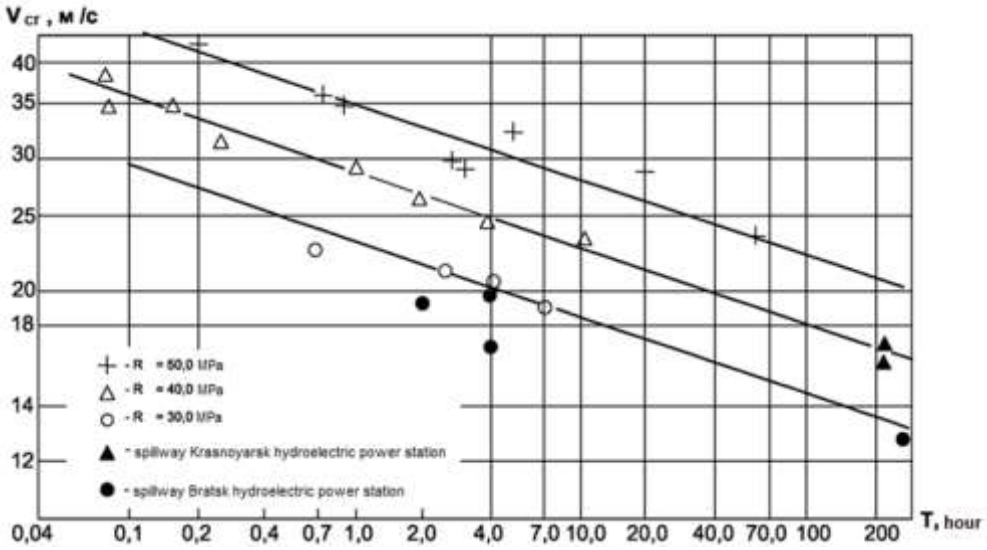

Figure 16: Dependence of incubation period on critical water flow velocity and concrete strength (Galperin et al, 1977).

Correspondingly, for an incubation period different from 48 hours, the critical velocity is determined by the formula:

The incubation period of the facing material can be increased by:

- Using high-strength concrete;
- Using aggregate with a size not exceeding 40 mm;
- Applying polymer or steel coatings.

4. Protection Of The Spillway Surface From Cavitation Erosion By Limiting The Height Of Maximum Unprocessed Offset

The following engineering measures to eliminate cavitation-prone defects formed on the surface during construction will contribute to protecting the concrete spillway surface from cavitation erosion

- Local protruding roughness (ridge-like deposits, reinforcement protrusions, embedded details) should be removed or cut flush with the adjacent surface;
- Local depressions (pits, cavities, areas of unprocessed concrete) should be patched flush with the adjacent surface$

For the most cavitation-prone typical surface roughness (offsets into the flow and offsets away from the flow), the maximum allowable height should be determined, and all offsets higher than this limit should be smoothed at a certain angle to eliminate cavitation damage. The cavitation indexes at the incipient damage for offsets with an inclined facet were obtained during field tests at the Bratsk HPP (Russia) (Galperin *et al*, 1977) and are presented in Table 2.

The maximum allowable height of the offset against the flow must satisfy two conditions:

- Condition 1: Avoidance of the erosion-prone cavitation stage $\sigma \geq 0.9 \quad (\sigma/\sigma_i \geq 0.45)$;
- Condition 2: Velocity at the height of the unprocessed protrusion $V_z \leq V_{cr}$ for the adopted surface facing material and air content in the flow near it.

In the first case, the hydraulic characteristics of the flow are determined for the calculated section: V_∞, P, u_*. Then, using the formula (1) for σ = 0.9, the permissible velocity V_{z0} is found, and for this velocity, using formula (10), is determined z_0/k_s, where z_0 the maximum allowable the height of the offset. Knowing the equivalent sand grain roughness Nikuradzse k_s, the calculated value is determined z_0.

Figure 17 presents the results of calculations using the proposed methodology for maximum velocities in the calculated sections of tunnels located at different distances x from the inlet with k_s = 1.0 mm and a maximum allowable height of a single offset into the flow z_0 = 5.0 mm. From the figure, it can be seen that the further the calculated section is from the inlet, the higher the maximum velocity that can be allowed in the current water without fearing cavitation.

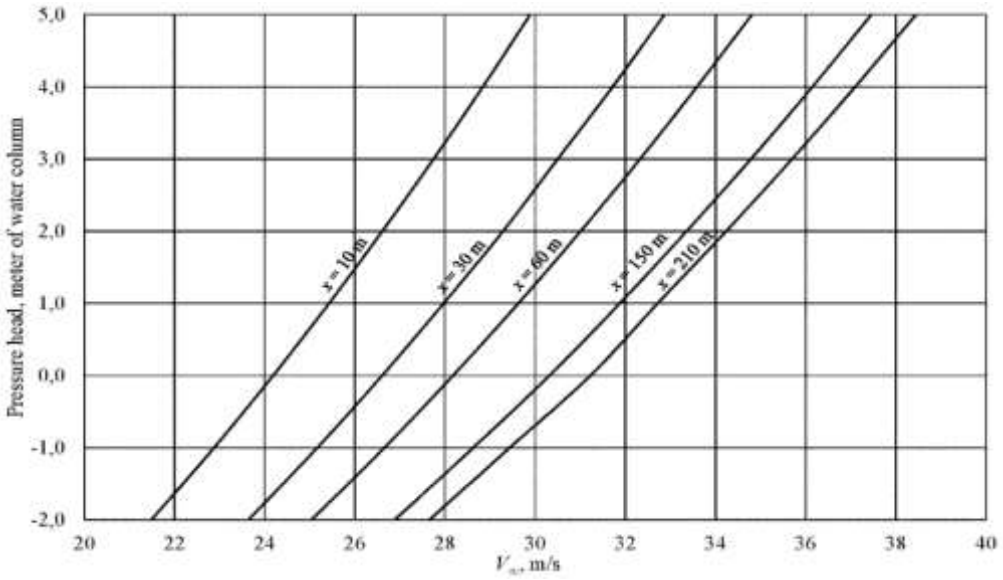

Figure 17: Allowable maximum velocities V_∞ in calculated sections from the condition (1): $\sigma = 0.9$, $z_0 = 5.0$ mm, $k_s = 1.0$ mm.

According to Condition 2, the velocity at the height of the allowable offset z_0 is equated to the critical velocity for the given surface facing material, depending on the flood duration and air content in the flow near the surface (Novikova *et al*, 1976; 1995). Subsequently, is determined from the logarithmic velocity distribution law (formula 10) z_0/k_s, and then, the permissible height of the protrusion z_0. Figure 18 presents calculated dependencies for determining the allowable maximum velocity in the calculated section obtained from Condition 2.

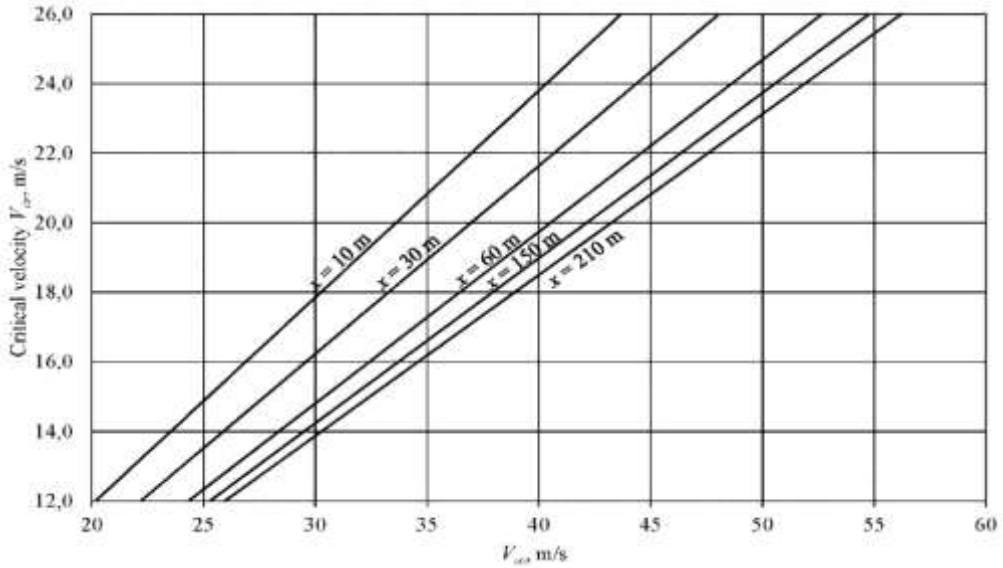

Figure 18: Allowable maximum velocities V_∞ in calculated sections from the condition (2): $V_z \leq V_{cr}$, $z_0 = 5.0$ mm, $k_s = 1.0$ mm.

Aeration systems, facilitating forced water flow, permit the acceptance of maximum velocities on concrete surfaces in spillway structures up to 50-55 m/s. The methodology proposed in this study was employed to calculate surface quality requirements for various spillways, including the operational spillway of the Sayano-Shushenskaya HPP (230 m height) and the Teri hydro complex in India (240 m height). The protection of the surfaces of these spillways is organized through the use of an aerator system.

Figure 19 depicts the arrangement of aerators on the surface of the open spillway of the Teri hydrocomplex.

Figure 19: Surface flow of the Teri HPP (India), equipped with aerator trampolines.

Figure 20 presents a schematic diagram of the operational spillway at the Sayano-Shushenskaya HPP, featuring aerator trampolines. Figure 21 provides a photo of the end section of the spillway in the 45th section. This stretch operated with the gate fully open for 18 years, totaling 230.3 days, and continuously for 21 days in 2003. The remaining eight sections of the dam operated from 1985 to 2003, averaging 126.4 days each, without any significant cavitation damage observed on their spillway surfaces, despite flow velocities at the spillway toe exceeding 55 m/s.

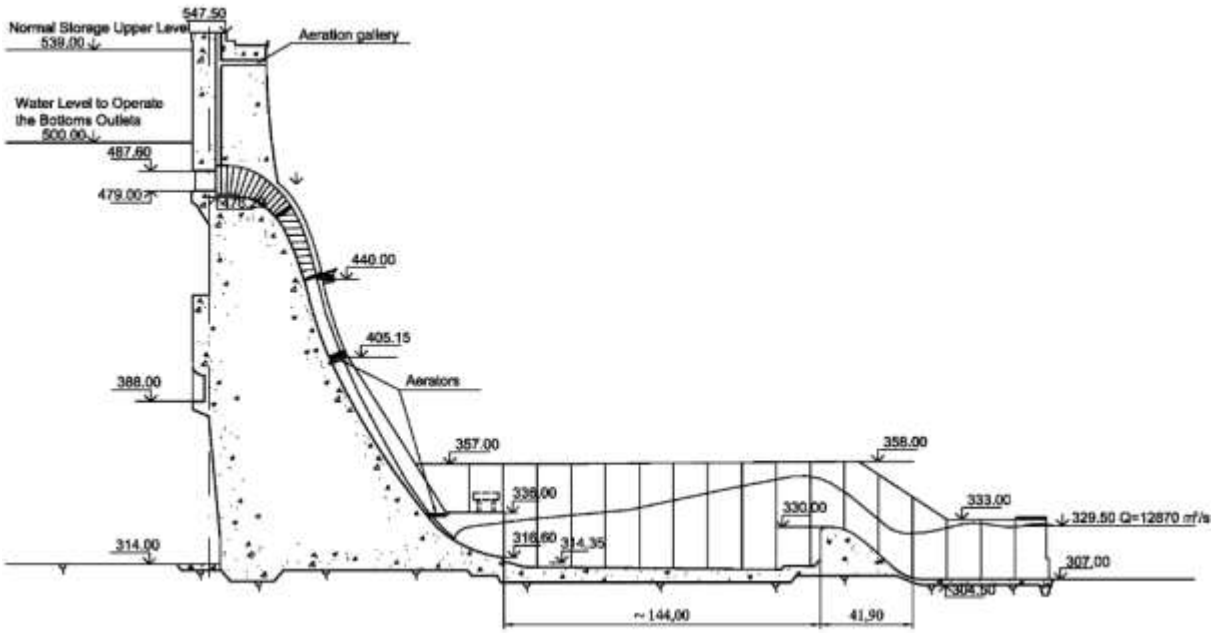

Figure 20: Schematic of the operational spillway at the Sayano-Shushenskaya HPP (Russia) with aerator trampolines.

Figure 21: Sayano-Shushenskaya HPP, Russia. Spillway Section 45 after 230 Days of Operation with Flow Velocities Exceeding 55 m/s.

Table 1: Cavitation Danger Levels Depending on the Cavitation Index.

Cavitation Index	Presence of Cavitation Erosion	Risk Level
$\sigma > 1.0$	No cavitation erosion	Level 0
$0.88 < \sigma \leq 1.0$	Point cavitation erosion, low intensity	Level 1
$0.70 < \sigma \leq 0.88$	Traces of cavitation impact with length less than 2.5 z_0, medium intensity	Level 2
$0.5 < \sigma \leq 0.70$	Length of primary surface damage area up to 10 z_0, maximum intensity	Level 3
$0.23 \leq \sigma \leq 0{,}50$	Length of primary surface damage area increases to 20 z_0, intensity decreases	Level 4
$\sigma < 0.23$	Jet flow, no closure of cavitation flame on the surface, no surface erosion	Level 0

Table 2: Cavitation index at the onset of erosion.

Slope ratio	Type of irregularity		
	Offset into flow	Offset away from flow	Longitudinal offset
1:2	1,00	-	Up to 0,40
1:3	-	-	0,33
1:4	-	-	0,27
1:5	0,62	0,66	
1:7	0,55	0,59	
1:10	0,49	0,53	
1:12	0,45	0,50	
1:15	0,41	0,45	
1:18	0,38	0,38	0,42
1:20	0,36	0,36	0,40
1:25	0,31	0,31	0,35
1:27	0,29	0,29	0,33
1:30	0,27	0,27	0,31

CONCLUSION

The presented study focuses on investigating the underlying causes and conditions leading to cavitation erosion on the surfaces of spillway structures. An essential consideration for the onset of cavitation erosion on water-submerged surfaces with individual irregularities is not the average water flow velocity but rather the velocity within the boundary layer at the height of potential isolated irregularities. In water conduits featuring a slight slope, the development of the boundary layer intensifies with the increasing distance from the entrance to the calculated section. Consequently, the tolerance for a solitary protrusion of greater height without the risk of cavitation erosion on the surface is augmented.

The proposed methodology for determining cavitation indices and, consequently, acceptable isolated irregularities on the surface of the flow path provides a robust framework for

ensuring guaranteed cavitation safety for spillway structures. The material resilience to withstand cavitation effects during the water discharge period enables the utilization of wall layer aeration, allowing for the acceptance of maximum flow velocities in spillway structures up to 50-55 m/s. This conclusion finds empirical support in the operational experience of both the surface spillway at the Teri hydrocomplex (height 240 m) and the operational spillway at the Sayano-Shushenskaya HPP (height 230 m).

REFERENCES

1. Arndt R.E.A., Holl J.W., Bohn J.C., Bechtel W.T. Influence of Surface Irregularities on Cavitation Performance. Journal of Ship Research, 1979; 23(3): 157-170. https://doi.org/10.5957/jsr.1979.23.3.157.
2. Ball J.W. Cavitation from Surface irregularities in high velocity flow. Journal of Hydraulic Divisions, ASCE, 1975; 112(9): 1283-1297. https://doi.org/10.1061/JYCEAJ.0004612
3. Bauer W.J. Turbulent boundary layer on steep slopes. Transactions, ASCE, 1954; 119: 1212–1233. https://doi.org/10.1061/TACEAT.0006971.
4. Berman J.R. and Novikova I.S. Determination of inception cavitation parameters for 2-D bodies in boundless flow by means of cavitation tests in hydrodynamic tunnels. Proceedings International Symposium on Cavitation, Deauville, France, 1995; 373-377.
5. Best Practices in Dam and Levee Safety Risk Analysis Published Jointly by the U.S. Army Corps of Engineers and Bureau of Reclamation, 2019.
6. Birkhoff G., Plesset M. and Simmons N. Wall Effects in Cavity Flow - I. Quarterly of Applied Mathematics, 1950; 8(2): 151-168. https://www.jstor.org/stable/43633802.
7. Birkhoff G., Plesset M. and Simmons N. Wall Effects in Cavity Flow, - II. Quarterly of Applied Mathematics, 1950; 9(4): 413-421. https://www.jstor.org/stable/43633926.
8. Borden R.C., Colgate D., Legas J., Selander C.E. Documentation of Operation, Damage, Repair, and Testing of Yellowtail Dam Spillway. Bureau of Reclamation, Report No. REC-ERC-71-23, 1971; 76.
9. Burgi P.H., Moyes B.M., Gamble T.W. Operation of Glen Canyon Dam Spillways summer 1983. Proceedings of the Conference on Water for Resource Development, American Society of Civil Engineers, pp. 260-265, Coeur d'Alene, Idaho, 1984; 14-17.
10. Colgate D. Aeration mitigates cavitation in Spillway Tunnels. ASCE National Water Reasearch, Engineering Meeting, 1972; 24-28.

11. Chanson H. Drag reduction in Open Channel flow by Aeration and Suspended Loud. Journal of Hydraulic Research, 1994; 32(1): 87-101. https://doi.org/10.1080/00221689409498791.
12. Chow V.T. Open channel hydraulics. McGraw- Hill Book Comp. New York, N Y., 2009.
13. Demiroz E., Acatay T. Influence of Chamfers Away From Flow on Cavitation Inception. XXI Congress of the International Association for Hydraulic Research, Melbourne, Australia, seminar, 1985; 2,4.
14. Echávez G. Risk Analysis of Cavitation in Hydraulic Structures. World Journal of Engineering and Technology, 2021; 9: 614-623. https://DOI: 10.4236/wjet.2021.93043.
15. Efros D.A. Hydrodynamic theory of two-dimensional Cavity flow. DAN USSR, 1946; 51(14): 267-270.
16. Falvey H.T. Cavitation in chutes and Spillways. Engineering monograph NO 42, United State Department of the Interior –Bureau of Reclamation, Denver, Colorado, 1990.
17. Galperin R.S., Oskolkov A.G., Semenkov V.M., Tsedrov G.N. Cavitation in hydraulic structures. Moscow: Energiya, 1977.
18. Gilbarg D. & Rock, D.H. On two theories of plane potential flow with finite cavities, U.S. Naval Ordnance Lab. Mem, 1946; 8718.
19. Houston K. L., Quint R. J., Rhone T. J. An Overview of Hoover Dam Tunnel Spillway Damage, Waterpower 85, Proceedings of an International Conference on Hydropower, American Society of Civil Engineers, 1985; 1421-1430.
20. Jin T., Liu C., Liu X. Cavitation inception of gate slots. U.S. Department of the Interior, Bureau of Reclamation, Engineering and Research Center, Division of Foreign Activities, 1985.
21. Kenn M.J. & Garrod A.D. Cavitation damage and the Tarbela Tunnel collapse of 1974. Prm. Instn Civ. Engrs, Part 1, 1981, 70, Nov., 779-810. https://doi.org/10.1680/iicep.1981.2075.
22. Kermani E.Fadaei, Barani G.A. and Ghaeini-Hessaroeyeh M. Investigation of cavitation damage levels on spillways. World Applied Sciences Journal, 2013; 21(1): 73-78. https://doi: 10.5829/idosi.wasj.2013.21.1.2630.
23. Kermani E.Fadaei, Barani G.A. and Ghaeini-Hessaroeyeh M. Drought Monitoring and Prediction using K-Nearest Neighbor Algorithm. Journal of AI and Data Mining, 2017; 5(2): 319-325. https://doi.org/10.22044/jadm.2017.881.

24. Kermani E.Fadaei, Barani G.A. and Ghaeini-Hessaroeyeh M. Cavition Damage Prediction on Dam Spillway using Fuzzy-KNN Modeling. Journal of Applied Fluid Mechanics, 2018; 11(2): 323-329. https://doi: 10.29252/jafm.11.02.28356.
25. Khatsuria R.M. Hydraulics of Spillways and Energy Dissipators. Marcel Dekker, New York, USA, 2005.
26. Novikova I.S., Semenkov V.M., Rodionov V.B. Concrete resistance in cavitation conditions on the spillway surface Proceedings, International Symposium on Cavitation, Deauville, France, 1995; 1-6.
27. Novikova I.S., Tsedrov G.N., Zolotov L.A. Assessment of cavitation resistance of materials, Proceedings of the IAHR Symposium Two-phase flow and cavitation in power generation systems, Grenoble, Frnce, 1976; 215-247.
28. Oroville Dam Spillway Incident, Independent Forensic Team Report. January, 2018.
29. Rajasekhar P., Santhosh Y.V.G., Soma Sekhar S. Physical and Numerical Model Studies on Cavitation Phenomenon-A Study on Nagarjuna Sagar Spillway. International Journal of Recent Development in Engineering and Technology, 2014; 2(1).
30. Schlichting H. and Gersten K. Boundary-Layer Theory. 9th Edition. - Springer-Verlag, Berlin, Heidelberg, 2017; 814.
31. Semenkov V.M. Large capacity outlets and spillways. General Report. The 13th International Congress on Large Dams, New Delhi, India, 1979; 112.
32. Terrier S.C.O. Hydraulic performance of stepped spillway aerators and related downstream flow features. Thèse No 6989, École Polytechnique Fédérale de Lausanne. Suisse, 2016.
33. Voynov Yu.P., Kupriyanov V.P., Rodionov V.B. Reconstruction of the spillway of Karun I HPP. Scientific-technical and production collection: "Safety of energy structures" / JSC NIIES, 1998; 2-3: 79-88.
34. Wan W., Liu B., Raza A. Numerical Prediction and Risk Analysis of Hydraulic Cavitation Damage in a High-Speed-Flow Spillway. Hindawi, Shock and Vibration, 2018, Article ID 1817307, 11 pages. https://doi.org/10.1155/2018/1817307
35. Wood I.R. Uniform region of self-aerated flow. Journal of Hydraulic Engineering, 1983; 109(3): 447-461. https://doi.org/10.1061/(ASCE)0733-9429(1983)109:3(447).